Interaction of the herbicide glyphosate with its target enzyme 5-enolpyruvylshikimate 3-phosphate synthase in atomic detail

Ernst Schönbrunn*†‡, Susanne Eschenburg†§, Wendy A. Shuttleworth¶, John V. Schloss*, Nikolaus Amrhein‖, Jeremy N. S. Evans¶, and Wolfgang Kabsch§

*Department of Medicinal Chemistry, University of Kansas, Lawrence, KS 66045; §Max Planck Institute for Medical Research, Department of Biophysics, D-69120 Heidelberg, Germany; ¶School of Molecular Biosciences, Washington State University, Pullman, WA 99164-4660; and ‖Institute of Plant Sciences, Swiss Federal Institute of Technology, CH-8092 Zurich, Switzerland

Edited by Gregory A. Petsko, Brandeis University, Waltham, MA, and approved December 13, 2000 (received for review August 25, 2000)

Biosynthesis of aromatic amino acids in plants, many bacteria, and microbes relies on the enzyme 5-enolpyruvylshikimate 3-phosphate (EPSP) synthase, a prime target for drugs and herbicides. We have identified the interaction of EPSP synthase with one of its two substrates (shikimate 3-phosphate) and with the widely used herbicide glyphosate by x-ray crystallography. The two-domain enzyme closes on ligand binding, thereby forming the active site in the interdomain cleft. Glyphosate appears to occupy the binding site of the second substrate of EPSP synthase (phosphoenol pyruvate), mimicking an intermediate state of the ternary enzyme·substrates complex. The elucidation of the active site of EPSP synthase and especially of the binding pattern of glyphosate provides a valuable roadmap for engineering new herbicides and herbicide-resistant crops, as well as new antibiotic and antiparasitic drugs.

The enzyme 5-enolpyruvylshikimate 3-phosphate (EPSP) synthase (EC 2.5.1.19) is the sixth enzyme on the shikimate pathway, which is essential for the synthesis of aromatic amino acids and of almost all other aromatic compounds in algae, higher plants, bacteria, and fungi (1–3), as well as in apicomplexan parasites (4). Because the shikimate pathway is absent from mammals (2, 3), EPSP synthase is an attractive target for the development of new antimicrobial agents effective against bacterial, parasitical, and fungal pathogens. A valuable lead compound in the search for new drugs and herbicides is glyphosate, which has proven as potent and specific inhibitor of EPSP synthase (5). Glyphosate is successfully used as a herbicide, being the active ingredient of the widely used weed control agent Roundup, and was recently shown to inhibit the growth of the pathogenic parasites *Plasmodium falciparum* (malaria), *Toxoplasma gondii*, and *Cryptosporidium parvum* (4).

EPSP synthase catalyzes the transfer of the enolpyruvyl moiety from phosphoenol pyruvate (PEP) to shikimate-3-phosphate (S3P) forming the products EPSP and inorganic phosphate (Scheme 1) (1, 6). The reaction is chemically unusual because it proceeds via C–O bond cleavage of PEP rather than via P–O bond cleavage (7) as in most PEP-utilizing enzymes. Glyphosate inhibits EPSP synthase in a slowly reversible reaction, which is competitive versus PEP and uncompetitive versus S3P (5, 8, 9).

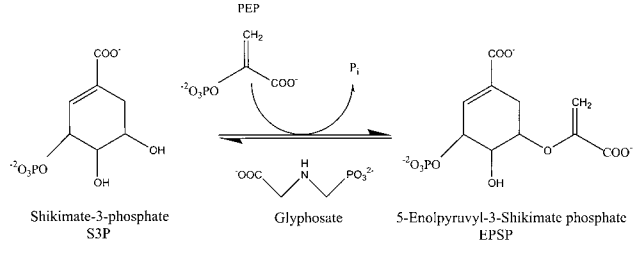

EPSP synthase (M_r 46,000) folds into two similar domains (10) (Fig. 1), each comprising three copies of a $\beta\alpha\beta\alpha\beta\beta$-folding unit. The only other enzyme known to exhibit this architecture is the mechanistic homologue UDP-*N*-acetylglucosamine enolpyruvyl transferase (MurA, EC 2.5.1.7) (11), which catalyzes the transfer of the intact enolpyruvyl moiety of PEP to a sugar nucleotide. MurA is essential for the synthesis of the bacterial cell wall and is the target of the broad spectrum antibiotic fosfomycin (12). On sugar nucleotide binding, MurA undergoes large conformational changes leading to the formation of the active site (13–16).

Although EPSP synthase has been extensively studied over more than three decades (17), conclusions on the enzyme mechanism (8, 9, 17, 18) and especially on the mode of action of the herbicide glyphosate (9, 17, 18) remained controversial. Up to now, the three-dimensional structure of EPSP synthase was only known in its unliganded form (10, 17), which does not reveal the active site of the enzyme. We have co-crystallized EPSP synthase with S3P and glyphosate as well as with S3P alone and determined the structures of these complexes at 1.5 and 1.6 Å resolution, respectively.

Methods

Catalytically competent EPSP synthase from *Escherichia coli* was purified following standard procedures (19). EPSP synthase in 50 mM Na-K-phosphate buffer, 1 mM DTT (pH 6.8) was concentrated to 100 mg/ml (about 2 mM) using Centricon 30 concentration devices (Amicon) at 4°C. Crystallization was performed at 20°C using the hanging-drop vapor-diffusion procedure. EPSP synthase was crystallized from 1 M Na-formate/25 mM Na-K-phosphate buffer (pH 7) in the presence of 5 mM S3P or 5 mM S3P and 5 mM glyphosate. Attempts to crystallize EPSP synthase in the absence of S3P under otherwise identical conditions failed.

Diffraction data were collected from flash-frozen crystals by the rotation method and recorded by a RaxisIV detector [x-rays: CuKα, focused by mirror optics (Molecular Structure Corporation, Houston, TX); generator: RU300 (Rigaku)]. Data processing, molecular replacement and refinement, and model building were performed with the program packages XDS (20), CNS

This paper was submitted directly (Track II) to the PNAS office.

Abbreviations: EPSP, 5-enolpyruvylshikimate 3-phosphate; PEP, phosphoenol pyruvate; S3P, shikimate-3-phosphate.

Data deposition: The atomic coordinates have been deposited in the Protein Data Bank, www.rcsb.org (PDB ID codes 1G6S and 1G6T).

†E.S. and S.E. contributed equally to this work.

‡To whom reprint requests should be addressed. E-mail: eschoenb@eagle.cc.ukans.edu.

The publication costs of this article were defrayed in part by page charge payment. This article must therefore be hereby marked "*advertisement*" in accordance with 18 U.S.C. §1734 solely to indicate this fact.

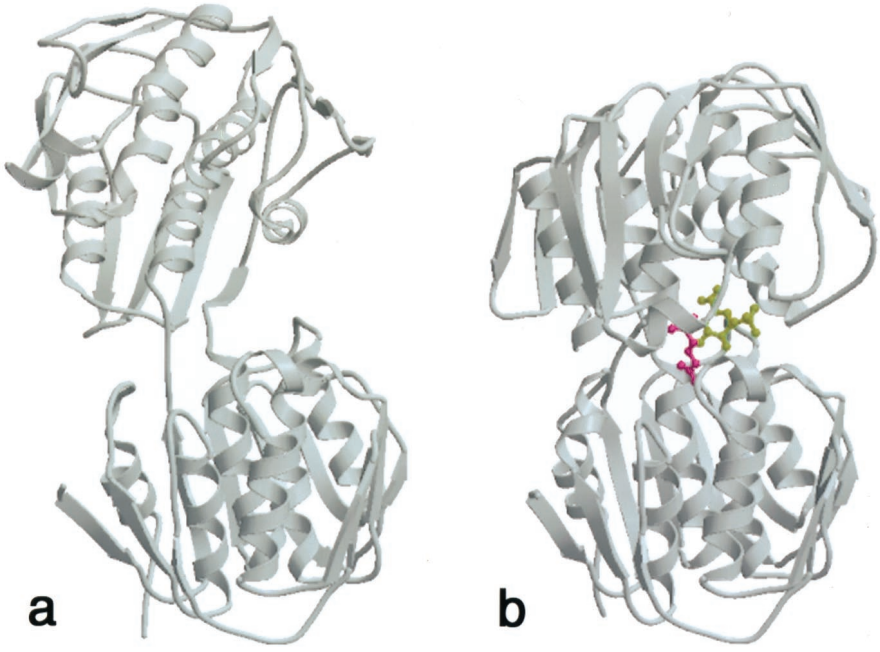

Fig. 1. Cartoon of EPSP synthase in the open and closed conformation. Top domain, residues 20–240; bottom domain, residues 1–19 plus 241–427. (*a*) Unliganded state (open) as reconstructed from the deposited α-carbon atoms (Protein Data Bank entry code 1EPS). (*b*) Liganded state (closed). S3P and glyphosate are shown as ball-and-stick models in green and magenta, respectively. Drawn with BOBSCRIPT (24).

(21), and O (22), respectively. A full-atom starting model of unliganded EPSP synthase was reconstructed with XCHAIN (23) from the deposited Cα atoms (Protein Data Bank entry code 1EPS), stereochemically refined using CNS, and subsequently split into two sets (residues 20–241 and 1–19 plus 242–427). These independent search models for the upper and lower domain of the EPSPS·S3P·glyphosate structure revealed clear signals in the cross-rotational and translational searches with data between 20 and 4.5 Å resolution. After initial rigid-body minimization, all subsequent refinements of the model were performed using data to highest resolution with no σ cut-off applied. Solvent molecules were added to the model at chemically reasonable positions. S3P, glyphosate, and ions were modeled unambiguously into the electron density maps. The EPSPS·S3P structure was solved using the protein part of the final EPSPS·S3P·glyphosate model. Data collection and refinement statistics are summarized in Table 1.

Results and Discussion

Comparing our structures of liganded EPSP synthase with the previously published Cα coordinates of the unliganded enzyme (Protein Data Bank entry code 1EPS; ref. 10), we find that the two domains of EPSP synthase approach each other in a screw-like movement, with the active site emerging in the

Table 1. Summary of data collection and refinement

Crystal	EPSPS·S3P	EPSPS·S3P·glyphosate
Space group	$P2_12_12_1$	$P2_12_12_1$
Unit cell dimensions	$a = 58.0$, $b = 84.9$, $c = 87.6$	$a = 57.8$, $b = 85.2$, $c = 88.1$
Molecules/asym. unit	1	1
Resolution range (Å)	20.0–1.60 (1.65–1.60)	20.0–1.50 (1.55–1.50)
Measured reflections	182207 (12801)	301724 (15899)
Unique reflections	57052 (4837)	67452 (6509)
Completeness (%)	98.7 (95.7)	96.0 (89.2)
R_{sym}* (%)	4.9 (18.1)	3.8 (13.6)
Protein atoms	3232	3232
Alternate atoms positions	58	60
Ligand atoms	16	26
Solvent molecules	555	599
Formate ions	13	10
Phosphate ions	1	0
R_{cryst}† (%)	15.5	15.0
R_{free}‡ (%)	18.6	17.1

Values in parentheses refer to the highest resolution shell.

*$R_{sym} = 100 \times \Sigma_h\Sigma_i|I_{hi} - I_h|/\Sigma_{hi}I_{hi}$ where h are unique reflection indices.

†$R_{cryst} = 100 \times \Sigma|F_{obs} - F_{model}|/\Sigma F_{obs}$ where F_{obs} and F_{model} are observed and calculated structure factor amplitudes, respectively.

‡R factor calculated for 3% randomly chosen reflections, which were excluded from the refinement.

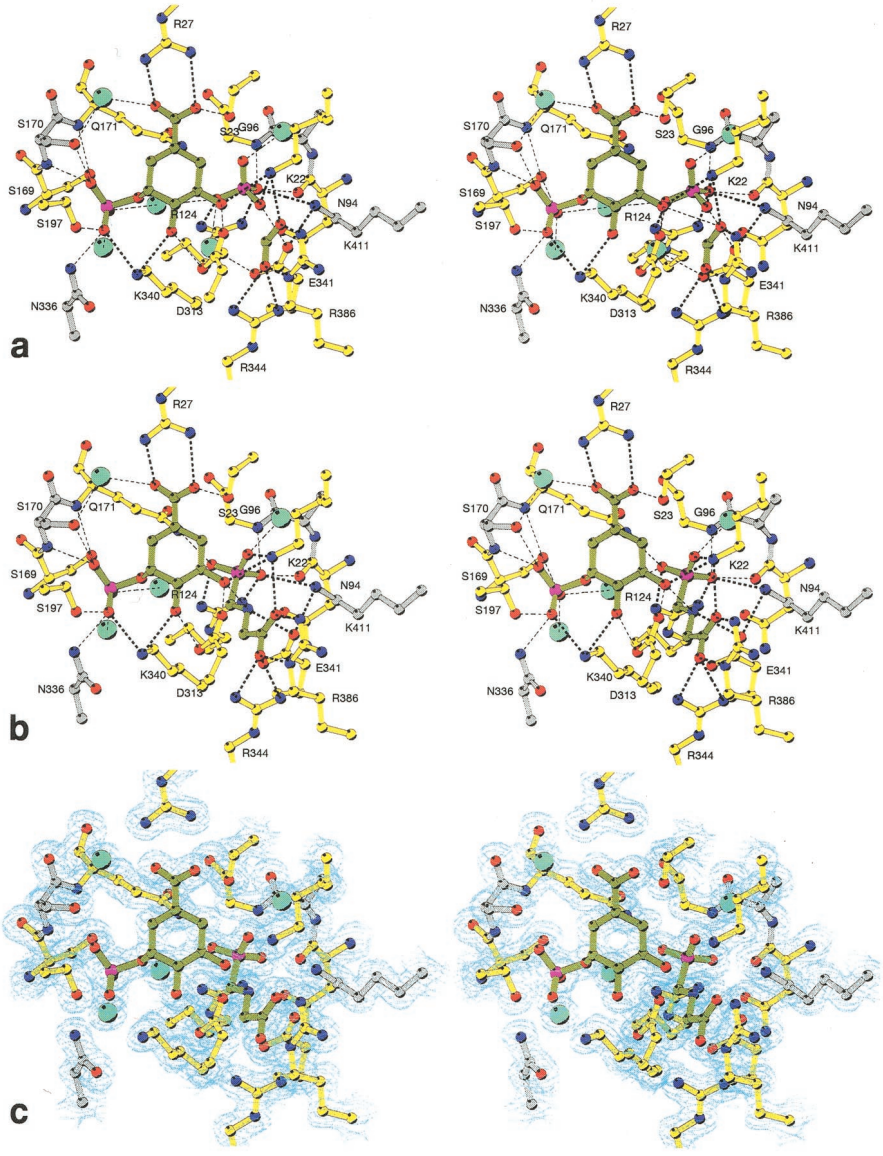

Fig. 2. The active site in S3P-liganded EPSP synthase. Strictly conserved residues are highlighted yellow. Noncarbon atoms are color-coded with blue for nitrogen, red for oxygen, and magenta for phosphorus. Light-blue spheres designate solvent molecules. Hydrogen bonds and ionic interactions are indicated by thin and thick dashed lines, respectively. Tyr-200, which is in hydrophobic contact with the cyclohexenyl moiety of S3P, is not shown. (*a*) In the absence of glyphosate (stereo view). S3P, formate, and phosphate are shown in green. (*b*) In the presence of glyphosate (stereo view). S3P and glyphosate are shown in green. (*c*) Final $2F_o - F_c$ electron density map of the EPSP synthase·S3P·glyphosate complex to 1.5-Å resolution contoured at 1σ (stereo view). Drawn with BOBSCRIPT (24).

interdomain cleft (Fig. 1). Glyphosate binds close to S3P (Fig. 2*b*) without perturbing the structure of the active-site cavity established in our inhibitor-free EPSP synthase·S3P complex (Fig. 2*a*). Distances between glyphosate, S3P, and surrounding protein side chain atoms are in good agreement with those predicted from solid-state NMR data (25, 26). The 5-hydroxyl group of S3P is hydrogen bonded to the nitrogen atom of glyphosate (Figs. 2*b* and 3). Two additional interactions between substrate and inhibitor are mediated through the side chain of Lys-22 and water molecule W2. The glyphosate binding site is dominated by charged residues from both domains of the enzyme, of which Lys-22, Arg-124, and Lys-411 have previously been implicated in PEP binding (27). In the absence of glyphosate from otherwise identical crystallization conditions (see *Methods*), a phosphate and a formate ion (Fig. 2*a*) occupy the positions of the phosphonate and carboxyl groups of glyphosate. However, the overall structure of this EPSP synthase·S3P complex is virtually identical with that of the EPSP synthase·S3P·glyphosate complex, representing the closed state of the enzyme. Because S3P appears to be essential for crystal formation in the used 1 M Na-formate/25 mM Na-K-phosphate (pH 7), we propose that it is S3P that triggers the enzyme's transition from the open to the closed state and not the negatively charged ions or glyphosate. Domain closure would lead to an accumulation of positive charges in the cleft attracting negatively charged molecules to the active site cavity. The proposed ordered mechanism, in which S3P binding is a prerequisite for glyphosate binding, is corroborated by the finding that the substitution of alanine for Arg-27, a residue that interacts exclusively with S3P (Figs. 2 and 3), prevents both the binding of S3P and that of glyphosate (27).

The formate and phosphate ions in the glyphosate-free structure (Fig. 2*a*) are coordinated by the same salt bridges

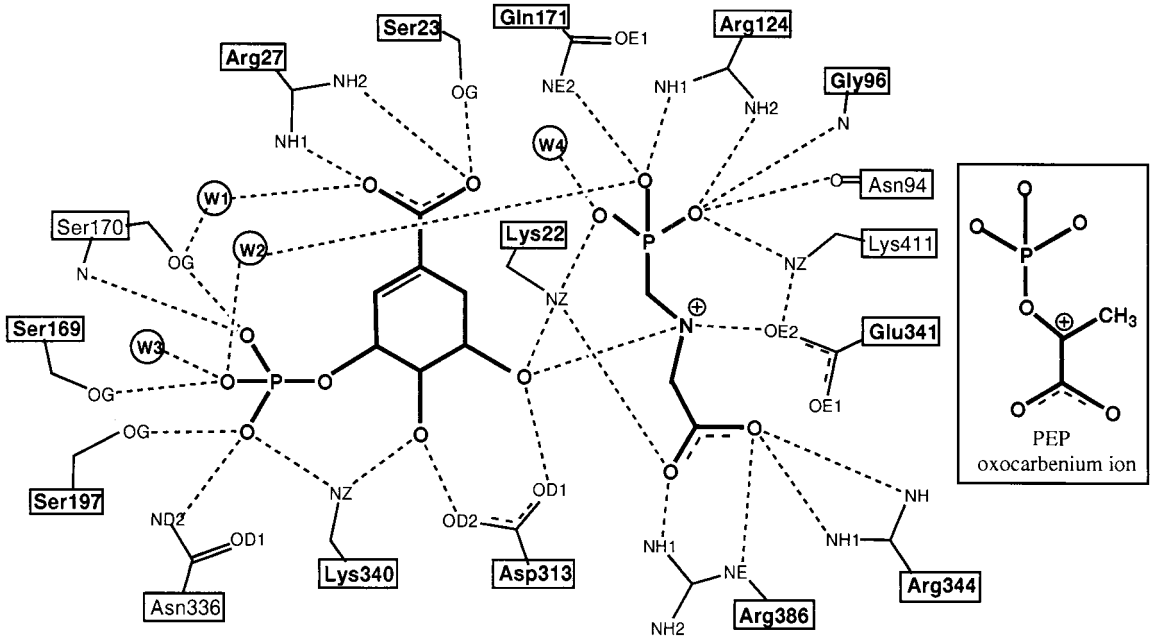

Fig. 3. Schematic representation of ligand binding in the EPSP synthase·S3P·glyphosate complex. Ligands are drawn in bold lines. Dashed lines indicate hydrogen bonds and ionic interactions. Strictly conserved residues are highlighted by bold labels. Protein atoms are labeled according to the Protein Data Bank nomenclature. Circled labels W1 to W4 designate solvent molecules. Hydrophobic interactions between S3P and Tyr-200 are omitted.

that bind the anionic centers of glyphosate (Figs. 2*b* and 3), suggesting that the phosphate and carboxyl moieties of PEP should exhibit the same ionic interactions. Clearly, the anionic centers of PEP are closer to each other than in the extended glyphosate conformation observed in our structure. Assuming that the carboxyl moieties of PEP and glyphosate are in the same position, the side chains of Lys-22, Arg-124, and Lys-411 must follow the phosphate group of the shorter PEP. The crystal structures indicate that the stretching of Arg-124 and slight rearrangements of the two lysine side chains required to maintain the interaction network are easily possible. This proposal is in line with the properties of the glyphosate-tolerant mutant protein Gly96Ala (28). The additional methyl group of the mutant would clash with the phosphonate group of glyphosate but would interfere less with the more remote phosphate group of PEP. Further evidence for a shared binding site between PEP and glyphosate in EPSP synthase comes from structural comparison with the mechanistically related (29) MurA. Comparing the glyphosate binding site of EPSP synthase with that part of the active site of MurA that binds the PEP moiety of the fluorinated analogue of MurA's tetrahedral reaction intermediate (Protein Data Bank entry code 1A2N; ref. 30), we identify the strictly conserved residues Lys-22, Arg-120, Asp-305, Arg-331, Arg-371, and Arg-397, which coordinate the PEP moiety in MurA, as corresponding to Lys-22, Arg-124, Asp-313, Arg-344, Arg-386, and Lys-411, respectively, of EPSP synthase. Thus, our results provide evidence that glyphosate occupies the PEP binding site, and they appear to rule out a recently suggested allosteric action of the herbicide (17, 18).

With the proposed position of PEP, Glu-341 could act as proton donor for the methylene group of PEP; proton addition would then proceed stereospecifically from the 2-*si* face of PEP consistent with previous findings (29). One carboxyl oxygen of Glu-341 could stabilize the incipient PEP oxocarbenium ion, as it would be in sub-van-der-Waals distance to C-2 of the carbocation. The side chain of Glu-341 is held in place through interactions with the backbone nitrogen of Glu-341 and with the side chains of Lys-411 and His-385. His-385 (distance His-385 NE2 − Glu-341 OE2 = 2.85 Å) is likely to function as proton source for Glu-341. Mutations of Lys-411 to Arg (27) and of His-385 to Lys, Ala, Gln, and Asn (31–33) result in a drastic decrease in the catalytic efficiency of the enzyme. The 5-hydroxyl group of S3P has to be deprotonated to attack the C-2 of PEP (34). In our structures, the 5-hydroxyl interacts with Asp-313 and Lys-22. Asp-313 probably acts as proton acceptor, whereas Lys-22 could protonate the oxygen of the scissile bond to facilitate the formation of inorganic phosphate.

The similarity between the two enolpyruvyl transferases EPSP synthase and MurA, pointed out above, appears to extend to details of the induced-fit mechanism. The MurA residues Arg-91, Asp-231, and Asp-369, thought to ease the transition from the open to the closed state of this enzyme (14–16), map to Arg-100, Asp-242, and Asp-384 of EPSP synthase, respectively. As shown for the substitutions R100A, D242A, and D384A (27), mutation of these residues drastically decreases EPSP synthase activity. Because none of these residues is involved in substrate binding, it is possible that the mutations hinder domain closure. By exploiting the analogy between EPSP synthase and MurA, the now available three-dimensional information on these two important drug targets should guide biochemical experiments to further clarify the unusual reaction principles of enolpyruvyl transfer and the associated induced-fit mechanism. In designing novel antimicrobial and herbicidal agents, it could be useful to construct molecules that block domain closure vital for the function of both enzymes.

We thank Ken Holmes (Max Planck Institute for Medical Research, Heidelberg, Germany) for generously supporting this work, Karolin Luger (Colorado State University, Ft. Collins, CO) for letting us use the crystallographic facilities at Colorado State University, and Andreas Becker (Max Planck Institute for Medical Research) for helpful discussions.

1. Bentley, R. (1990) *Crit. Rev. Biochem. Mol. Biol.* **25,** 307–383.
2. Haslam, E. (1993) *Shicimic Acid: Metabolism and Metabolites* (Wiley, Chichester, U.K.).
3. Kishore, G. M. & Shah, D. M. (1988) *Annu. Rev. Biochem.* **57,** 627–663.
4. Roberts F., Roberts, C. W., Johnson, J. J., Kyle, D. E., Krell, T., Coggins, J. R., Coombs, G. H., Milhous, W. K., Tzipori, S., Ferguson, D. J. P., *et al.* (1998) *Nature (London)* **393,** 801–805.
5. Steinrücken, H. C. & Amrhein, N. (1980) *Biochem. Biophys. Res. Commun.* **94,** 1207–1212.
6. Levin, J. G. & Sprinson, D. B. (1964) *J. Biol. Chem.* **239,** 1142–1150.
7. Walsh, C. T., Benson, T. E., Kim, D. H. & Lees, W. J. (1996) *Chem. Biol.* **3,** 83–91.
8. Boocock, M. R. & Coggins, J. R. (1983) *FEBS Lett.* **154,** 127–133.
9. Steinrücken, H. C. & Amrhein, N. (1984) *Eur. J. Biochem.* **143,** 351–357.
10. Stallings, W. C., Abdel-Meguid, S. S., Lim, L. W., Shie, H.-S., Dayringer, H. E., Leimgruber, N. K., Stegemann, R. A., Anderson, K. S., Sikorski, J. A., Padgette, S. R. & Kishore, G. M. (1991) *Proc. Natl. Acad. Sci. USA* **88,** 5046–5050.
11. Schönbrunn, E., Sack, S., Eschenburg, S., Perrakis, A., Krekel, F., Amrhein, N. & Mandelkow, E. (1996) *Structure (London)* **4,** 1065–1075.
12. Kahan, F. M., Kahan, J. S., Cassidy, P. J. & Kropp, H. (1974) *Ann. N.Y. Acad. Sci.* **235,** 364–385.
13. Schönbrunn, E., Svergun, D. I., Amrhein, N. & Koch, M. H. J. (1998) *Eur. J. Biochem.* **253,** 406–412.
14. Schönbrunn, E., Eschenburg, S., Krekel, F., Luger, K. & Amrhein, N. (2000) *Biochemistry* **39,** 2164–2173.
15. Eschenburg, S. & Schönbrunn, E. (2000) *Proteins Struct. Funct. Genet.* **40,** 290–298.
16. Schönbrunn, E., Eschenburg, S., Luger, K., Kabsch, W. & Amrhein, N. (2000) *Proc. Natl. Acad. Sci. USA* **97,** 6345–6349. (First Published May 23, 2000; 10.1073/pnas.120120397)
17. American Chemical Society (1997). *Glyphosate: A Unique Global Herbicide* (American Chemical Society Monograph, Washington, D.C.).
18. Sikorski, J. A. & Gruys, K. J. (1997) *Acc. Chem. Res.* **30,** 2–8.
19. Shuttleworth, W. A., Hough, C. D., Bertrand, K. P. & Evans, J. N. S. (1992) *Protein Eng.* **5,** 461–466.
20. Kabsch, W. (1993) *J. Appl. Crystallogr.* **26,** 795–800.
21. Brünger, A. T., Adams, P. D., Clore, G. M., DeLano, W. L., Gros, P., Grosse-Kunstleve, W., Jiang, J.-S., Kuszewski, J., Nilges, M., Pannu, N. S., *et al.* (1998) *Acta Crystallogr. D* **54,** 905–921.
22. Jones, T. A., Zou, J.-Y., Cowan, S. W. & Kjeldgaard, M. (1991) *Acta Crystallogr. A.* **47,** 110–119.
23. Kabsch, W., Mannherz, H. G., Suck, D., Pai, E. F. & Holmes, K. C. (1990) *Nature (London)* **347,** 37–44.
24. Esnouf, R. M. (1997) *J. Mol. Graphics* **15,** 132–134.
25. McDowell, L. M., Klug, C. A., Beusen, D. D. & Schaefer, J. (1996) *Biochemistry* **35,** 5395–5403.
26. McDowell, L. M., Schmidt, A., Cohen, E. R., Studelska, D. R. & Schaefer, J. (1996) *J. Mol. Biol.* **256,** 160–171.
27. Shuttleworth, W. A., Pohl, M. E., Helms, G. L., Jakeman, D. L. & Evans, J. N. S. (1999) *Biochemistry* **38,** 296–302.
28. Sost, D. & Amrhein, N. (1990) *Arch. Biochem. Biophys.* **282,** 433–436.
29. Kim, D. H., Tucker-Kellogg, G. W., Lees, W. J. & Walsh, C. T. (1996) *Biochemistry* **35,** 5435–5440.
30. Skarzynski, T., Kim, D. H., Lees, W. J., Walsh, C. T. & Duncan, K. (1998) *Biochemistry* **37,** 2572–2577.
31. Shuttleworth, W. A. & Evans, J. N. S. (1994) *Biochemistry* **33,** 7062–7068.
32. Shuttleworth, W. A. & Evans, J. N. S. (1996) *Arch. Biochem. Biophys.* **334,** 37–42.
33. Majumder, K., Selvapandiyan, A., Fattah, F. A., Arora, N., Ahmad, S. & Bhatnagar, R. K. (1995) *Eur. J. Biochem.* **229,** 99–106.
34. Bondinell, W. E., Vnek, J., Knowles, P. F., Sprecher, M. & Sprinson, D. B. (1971) *J. Biol. Chem.* **246,** 6191–6196.